Journal of Alloys and Compounds 502 (2010) 396–400

Contents lists available at ScienceDirect

Journal of Alloys and Compounds

journal homepage: www.elsevier.com/locate/jallcom

Synthesis of gadolinium aluminate powder through citrate gel route

Amit Sinha [a,b,*], B.P. Sharma [a], H. Näfe [b], P. Gopalan [c]

[a] Energy Conversion Materials Section, Materials Group, Bhabha Atomic Research Centre, Vashi Complex, Navi Mumbai 400705, India
[b] Max-Planck-Institut für Metallforschung, Pulvermetallurgisches Laboratorium, Heisenbergstrasse 3, Stuttgart 70569, Germany
[c] Department of Metallurgical Engineering and Material Science, Indian Institute of Technology Bombay, Mumbai 400076, India

ARTICLE INFO

Article history:
Received 29 October 2009
Received in revised form 21 April 2010
Accepted 25 April 2010
Available online 5 May 2010

Keywords:
Gadolinium aluminate
GdAlO3
Citrate–nitrate
TG–DSC
HT-XRD
Mass spectrometry
Rietveld analysis

ABSTRACT

Nanocrystalline gadolinium aluminate ($GdAlO_3$) powder was prepared through citrate gel route. The thermal decomposition behavior of gadolinium–aluminium–citrate–nitrate precursor powder was studied with the help of thermo gravimetric analysis combined with differential scanning calorimetry and mass spectroscopy. The phase evolution of the powder at different temperatures was characterized by high-temperature X-ray diffraction. The decomposition of the precursor powder in oxidizing atmosphere was found to be a three-step process: (i) evolution of water and ammonia; (ii) evolution of carbon dioxide, residual water, and ammonia; (iii) oxidation of residual carbon. Calcination of precursor powder at 800 °C under static air was found to result in $GdAlO_3$ phase. In the absence of oxidizing atmosphere the amorphous precursor powder only partially crystallized into $GdAlO_3$ phase at 1200 °C.

1. Introduction

The development of rare earth based perovskite type oxides has a very promising future. Ceramics based on Ln_2O_3–Al_2O_3 (Ln–lanthanide element) system are promising materials for optical, magnetic, electronic and structural applications [1–3]. Many other perovskite aluminates find applications as host for solid-state lasers, luminescence systems, solid electrolytes, chemical sensors, magnetic refrigeration materials, substrates for high-temperature superconductor deposition, catalyst supports and thermal barrier coatings [4,5]. $GdAlO_3$ based perovskites have potential application as phosphor [6–8], scintillator [9], and regenerator material for sub-4 K cryo-coolers [10]. In our previous studies, it was observed that gadolinium aluminate ($GdAlO_3$) is a potential host for materials with oxygen ion conductivity [11,12].

$GdAlO_3$ belongs to the family of rare earth aluminates that crystallize in a slightly distorted orthorhombic perovskite structure. Conventionally $GdAlO_3$ is produced by solid-state reaction of Gd_2O_3 and Al_2O_3 [9]. The solid-state synthesis of rare earth based aluminates usually calls for an extensive mechanical mixing combined with lengthy heat treatments. These processing parameters do not permit a fine control over the morphology of powder particles and microstructure of the sintered body [13]. Several wet-chemical techniques, such as the polymerized complex route, combustion synthesis, sol–gel have been utilized to synthesize gadolinium aluminate ($GdAlO_3$) based perovskite powder [6,7,14–16]. Cizauskaite et al. [16] have recently reported preparation of $GdAlO_3$ powder using a sol–gel process that involves several heat treatments of Gd–Al–acetate–nitrate–glycolate precursor to yield $GdAlO_3$ powder. However, this process is not suitable for preparing powder for undoped as well as doped $GdAlO_3$ compositions as the $GdAlO_3$ powder produced through this route contained several impurity phases such as Gd_2O_3, $Gd_3Al_5O_{12}$ and $Gd_4Al_2O_9$.

The citrate gel route is one of the wet-chemical techniques for preparation of high-purity, homogeneous, multi-component ceramic powders [17]. The citrate gel route is similar to Pechini process [18], except that ethylene glycol or other poly-hydroxy alcohols are not added for esterification. Citric acid forms stable complexes with a host of metal ions. Thus addition of citric acid to multi-component metal nitrates yields a stable transparent gel on dehydration. Hence this process has been used to prepare a variety of multi-component oxide ceramic powders [19–25].

In our previous investigation, for singly and doubly doped $GdAlO_3$ compositions, the citrate gel route was found to produce powders that could be sintered to good densities at significantly lower temperatures compared to those prepared by conventional solid-state synthesis method [11]. In the present work, a systematic study has been carried out to investigate the thermal decomposition behavior of gadolinium aluminate citrate–nitrate precursor using thermal analysis coupled with mass spectroscopy.

* Corresponding author at: Energy Conversion Materials Section, Materials Group, Bhabha Atomic Research Centre, Vashi Complex, Navi Mumbai 400705, India.
Tel.: +91 22 27887161; fax: +91 22 27840032.
E-mail address: amit97@yahoo.com (A. Sinha).

0925-8388/$ – see front matter © 2010 Elsevier B.V. All rights reserved.
doi:10.1016/j.jallcom.2010.04.179

Table 1
Chemical composition of Gd–Al–nitrate–citrate precursor in wt.%, mol.% and normalized form.

Sample	wt.%	mol. %	No. of moles (normalized)	Form of conversion	No. of moles of 'O' required	Total 'O' required
Gd	32.55 ± 0.17	0.21	4.1	$GdO_{1.5}$	6.15	
Al	5.44 ± 0.03	0.21	4.1	$AlO_{1.5}$	6.15	
N	18.0 ± 0.05	0.05	1.0	NH_3	–	
H	2.64 ± 0.06	2.64	53	H_2O	25[a]	
C	40.5 ± 0.1	1.50	30	CO/CO_2	30/60	
O	0.69 ± 0.02	2.53	50.6	–		67.3/97.3

[a] Out of 53 'H' atoms, 3 'H' atoms are consumed for formation of NH_3.

The structural parameters of $GdAlO_3$ powder were studied using Rietveld refinement on XRD pattern of the calcined powder.

2. Experimental

$Gd(NO_3)_3{\cdot}9H_2O$ (99.99% purity, Indian Rare Earth, India), and $Al(NO_3)_3{\cdot}9H_2O$ (AR Grade, E-Merck India) were used as starting materials for the preparation of $GdAlO_3$ powder using citrate gel route. Equimolar amounts of Gd- and Al-nitrate solutions were mixed and the metal ions were complexed by adding sufficient citric acid (AR Grade, E-Merck, India). The mixed solution was slowly dehydrated on a laboratory hot plate to form a viscous gel. The gel was further dried at 130 °C for 2 h to yield precursor powder. Chemical composition of the gadolinium aluminate precursor powder was determined by optical emission and optical absorption spectrometry with inductively coupled plasma excitation (OES-ICP, JY 70 Plus, Instruments S.A., France). A hot-carrier-gas extraction method was used in a resistance furnace at $T > 2500$ °C, (TC-436 DR, LECO, USA) to determine the oxygen content. Thermo gravimetric (TG) analysis and differential scanning calorimetric (DSC) studies of the dried gel precursor of $GdAlO_3$ were carried out in a thermo balance (Netzsch STA 449C, Germany) in dynamic air atmosphere in an alumina crucible. The air flow rate was maintained at 73 ml min^{-1}. The weight loss as a function of temperature was recorded up to 1400 °C. The heating rate was 10 K/min from ambient temperature to 1400 °C. During TG–DSC measurement, the evolved gases were simultaneously analysed with the help of mass spectrometer (Balzers QMG 421, Germany). Based on the TG/DSC studies, the citrate gel derived precursor powder was calcined at 800 and 1000 °C for 2 h.

For phase analysis, calcined powders were characterized by X-ray diffraction (Philips Analytical, Model PW1710). Standard silicon sample was employed as internal standard for calibration. The XRD patterns were recorded at a scan rate of 0.025°/s using CuK_α radiation. High-temperature XRD (HT-XRD) data were obtained with a curved position solid-state detector (INEL CPS 120). The precursor powder taken for HT-XRD study was pre-calcined at 500 °C for 30 min under static air in order to ensure the removal of the major organic constituents from the structure. For HT-XRD, the powder sample was heated on a tantalum substrate under vacuum with a heating rate of 50 K/min in a high-temperature furnace and the XRD data were recorded in the temperature range of 600–1400 °C. The lattice parameters of $GdAlO_3$ powder, calcined at 1400 °C under static air, were determined through Rietveld refinement of high resolution XRD data. For this, high resolution XRD data were collected at a step interval of 0.0085 2θ and a step counting time of 10 s (Panalytical, Model: X'Pert Pro). Rietveld analysis was performed using Fullprof program incorporated in the WinPLOTR software package [26]. The morphology of the calcined $GdAlO_3$ powder was studied using scanning electron microscope (SERON AIS2100).

3. Results and discussion

3.1. Thermal analysis of $GdAlO_3$ citrate–nitrate precursor

During preparation of precursor powder by dehydration and drying of citrate–nitrate gel, the NO_x gases evolve. It would, therefore, be logical to expect that the resulting precursor powder would have rather uncertain composition. Hence, chemical composition of the precursor powder was determined (Table 1) so that a correlation can be achieved with the thermogravimetry data. The low nitrogen content in the precursor powder corroborates with the observation that NO_x gases evolve during gel drying. Based on the elemental analysis, the theoretical weight loss during thermal treatment of precursor powder to form $GdAlO_3$ will be 51.9%. The experimental weight loss during thermal analysis was 49.9%, which is quite close to the theoretical value.

Fig. 1 shows TG–DSC diagram of gadolinium aluminate citrate precursor. The decomposition of Gd–Al–nitrate–citrate precursor was found to be a three-step process. In the first step, the weight loss in the TG graph at 121 °C can be attributed to the evolution of

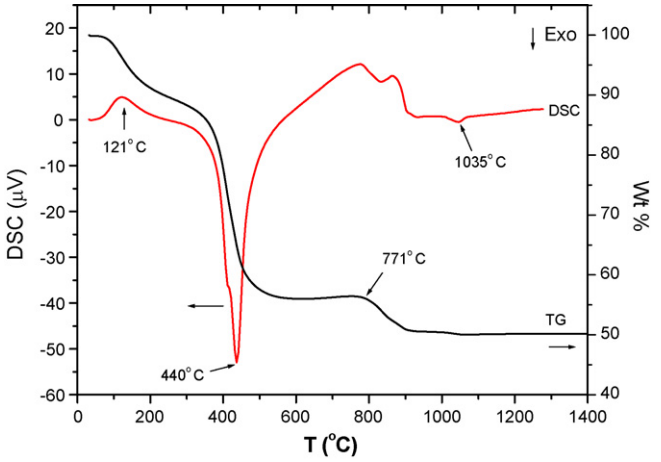

Fig. 1. TG–DSC diagram of gadolinium aluminate citrate precursor.

water molecule. This is confirmed by the appearance of endothermic peak in the DSC plot and the presence of H_2O peak in the mass spectrograph (Fig. 2). A small amount of NH_3 was also released during this stage.

In the second step, a major weight loss (34%) takes place in the temperature range of 237–560 °C. This is accompanied by the evolution of CO_2 and H_2O and small amounts of NH_3, NO, CH_3, CO and NO_2 (Fig. 3). This step can be attributed to the decomposition of citrate functional group.

In the third step (771–950 °C), oxidation of carbon takes place with the evolution of CO_2. At 1035 °C, a small exothermic peak was observed which was associated with insignificant weight change in the sample. This could be attributed to oxidation of residual carbon present in the powder. This corroborates with the presence of CO_2 peak in mass spectrograph (Fig. 2).

The chemical composition of the precursor powder can be converted into mol.%. Table 1 shows composition of the precursor in

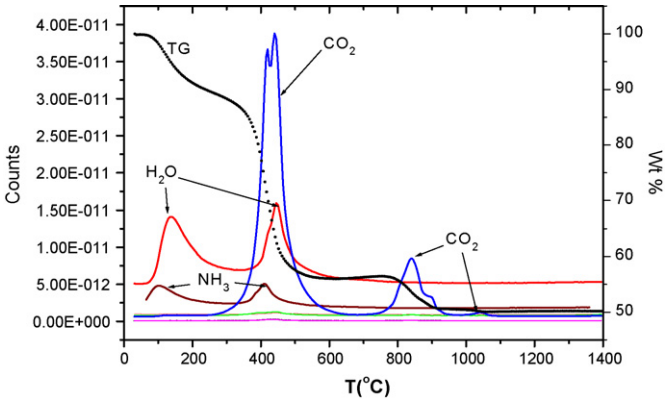

Fig. 2. TG diagram of gadolinium aluminate citrate precursor along with mass spectrogram for evolved gases.

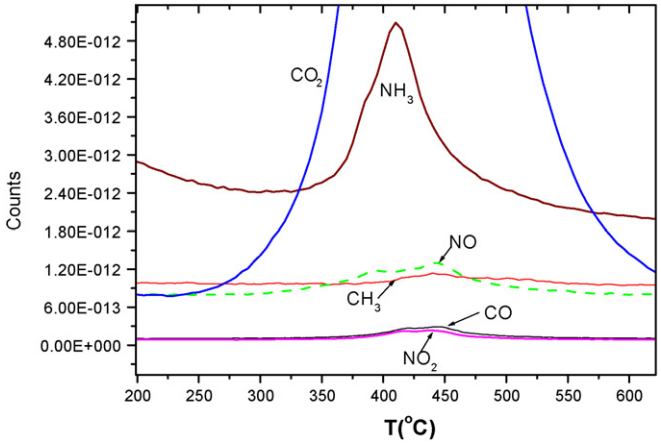

Fig. 3. Enlarged mass spectrogram for gases evolved during thermal treatment of gadolinium aluminate citrate precursor.

mol.% as well as in normalized form. MS diagrams revealed that the nitrogen leaves the powder mostly in the form of NH_3, whereas hydrogen is released as H_2O. Each mole of Al and Gd needs 1.5 moles of 'O' for conversion into respective oxides and subsequent formation of $GdAlO_3$. As per the mass spectrogram, carbon leaves the system mostly in the form of carbon dioxide. Thus there is significant deficit of oxygen in the precursor for the complete oxidation of carbon. Flowing air must be compensating for this deficit. Appearance of small exothermic peak in the DSC and CO_2 signal in mass spectrograph above 1000 °C can only be explained by oxidation of residual carbon trapped deep in the pores of the powder. The above results signify that the calcination of citrate gel derived precursor requires oxidizing atmosphere for its complete conversion to phase pure $GdAlO_3$. To confirm this point, phase evolution of the precursor powder was studied as a function of calcination temperature under oxidizing atmosphere as well as under low partial pressure of oxygen.

Chemical composition of the precursor was used to assign it a chemical formula: $Gd_{4.1}Al_{4.1}C_{30}H_{53}O_{50.6}N$. The TG–DSC–MS results were used to postulate the reaction steps during heating under dynamic air flow:

Step 1 (temperatures: RT–270 °C):

$$Gd_{4.1}Al_{4.1}C_{30}H_{53}O_{50.6}N \rightarrow Gd_{4.1}Al_{4.1}C_{30}H_{27.5}O_{38.6}N_{0.5} + 0.5NH_3 + 12H_2O \quad (1)$$

Step 2 (temperatures: 270–670 °C):

$$Gd_{4.1}Al_{4.1}C_{30}H_{27.5}O_{38.6}N_{0.5} + 12.35O_2 \rightarrow Gd_{4.1}Al_{4.1}C_{11}O_{12.3} + 0.5NH_3 + 13H_2O + 19CO_2 \quad (2)$$

Step 3 (temperatures: 670–1100 °C):

$$Gd_{4.1}Al_{4.1}C_{11}O_{12.3} + 11O_2 \rightarrow 4.1GdAlO_3 + 11CO_2 \quad (3)$$

The overall decomposition reaction of the precursor may be expressed as

$$Gd_{4.1}Al_{4.1}C_{30}H_{53}O_{50.6}N + 23.35O_2 \rightarrow 4.1GdAlO_3 + NH_3 + 25H_2O + 30CO_2 \quad (4)$$

3.2. XRD study of $GdAlO_3$ citrate–nitrate precursor

To study the phase evolution of the precursor powder in the absence of oxidizing atmosphere, *in situ* high-temperature X-ray diffraction patterns were recorded under a vacuum level better than 10^{-3} Pa. Fig. 4 shows the HT-XRD patterns of

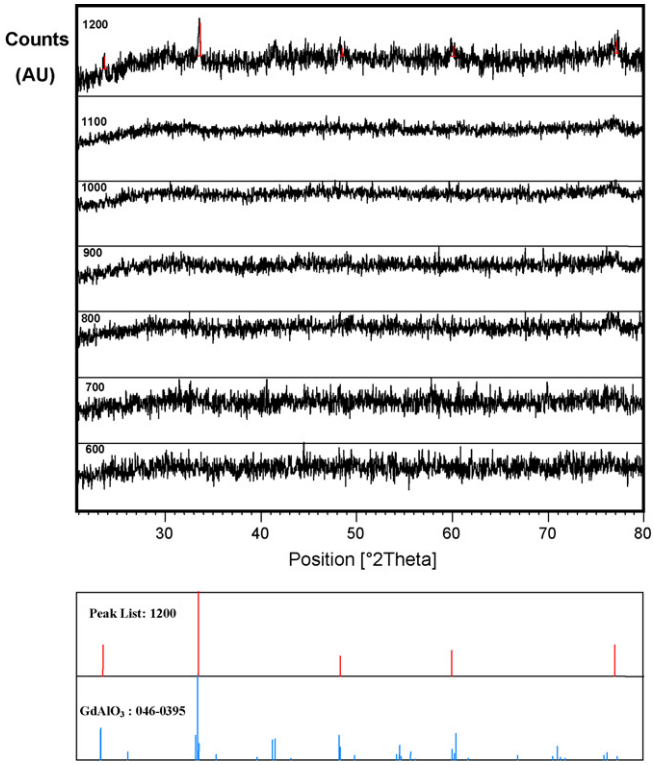

Fig. 4. High-temperature XRD patterns of gadolinium aluminate precursor powders recorded under low oxygen partial pressure in the temperature range of 600–1200 °C.

gadolinium–aluminium citrate–nitrate precursor powder recorded in the temperature range of 600–1200 °C. All the XRD patterns up to a temperature of 1100 °C show high background count without any characteristic reflections for $GdAlO_3$ phase. These results suggest that the powder did not crystallize into the desired phase even though the temperature was raised to 1100 °C. The major characteristic reflections corresponding to $GdAlO_3$ phase can only be observed in the XRD pattern recorded at 1200 °C. The high background count of this XRD pattern suggests the partial crystallization of the amorphous powder into $GdAlO_3$ as well as presence of residual carbon which was confirmed by the blackish color of the powder obtained after quenching it to room temperature under vacuum. The HT-XRD studies of the gadolinium–aluminium citrate–nitrate precursor powder confirms the results of TG/DSC/MS that complete decomposition of the precursor calls for oxidizing atmosphere.

Fig. 5a shows the XRD patterns of $GdAlO_3$ precursor powder calcined under static air at 800 °C. The pattern reveals major X-ray reflections corresponding to the strongest peaks of $GdAlO_3$ phase [ICDD PDF 46-0395]. The XRD pattern of precursor powder calcined at 1000 °C (Fig. 5b) exhibits all the reflections corresponding to orthorhombic crystal structure of $GdAlO_3$ phase. The crystallite size of the powder was calculated using Scherrer Formula. The $GdAlO_3$ powder was found to be nanocrystalline having a crystallite size of 18 nm.

3.3. Structural refinement through Rietveld method

In general, the Rietveld method utilises the least-squares refinement for obtaining the best fit between the experimental data and the calculated pattern based on the simultaneously refined models. In the present investigation, a Thomson–Cox–Hasting pseudo–Voigt peak profile function [27] was used for the profile fitting. The analysis was accomplished assuming Pnma space group

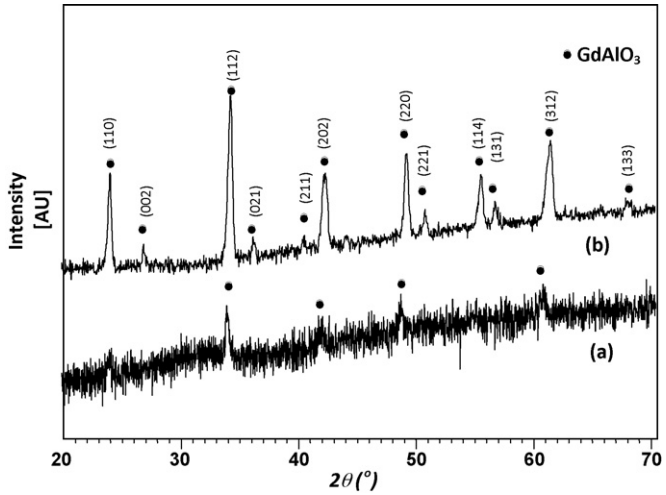

Fig. 5. Room temperature XRD patterns of gadolinium aluminate precursor powder calcined at (a) 800 and (b) 1000 °C for 2 h under oxygenated environment (air).

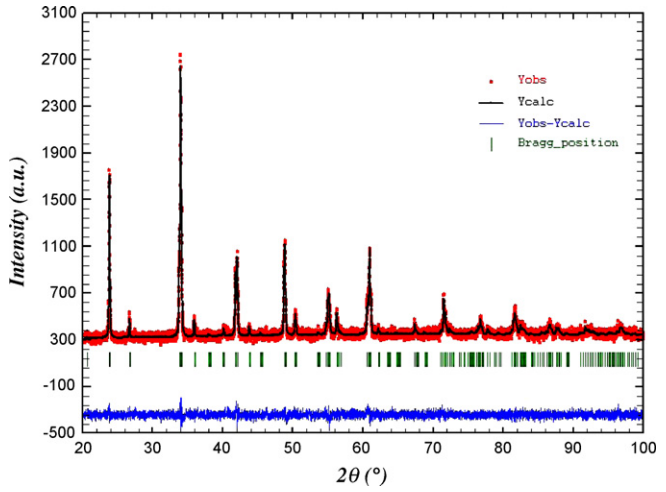

Fig. 6. Rietveld analysis result of $GdAlO_3$ powder. The calculated and observed patterns are shown in the top by the solid line and the dots respectively. The vertical marks in the middle show positions calculated for Bragg reflection. The trace in the bottom is a plot of the difference: observed minus calculated.

for distorted orthorhombic structure. The background was fitted with a sixth order polynomial function. Fig. 6 shows the Rietveld pattern of $GdAlO_3$ powder. The tick marks below the patterns represent the positions of all possible Bragg reflections. The lower solid line represents the difference between the observed and calculated intensities. The refined lattice parameters of $GdAlO_3$ are given in Table 2. The quality of the agreement between observed and calculated profiles is evaluated by profile factor (R_p), weighted profile factor (R_{wp}), and reduced chi-square (χ^2). The mathematical expressions of the above parameters can be found elsewhere [28,29]. The reliability parameters obtained for the presented analysis through this refinement were R_p: 4.62%; R_{wp}: 5.80%; R_{exp}: 5.18%; χ^2: 1.25. The lattice parameters obtained after Rietveld refinements are in good agreement with the reported values [ICDD PDF 046-0395]. Based on the refined structural parameters obtained through Rietveld analysis, the orthorhombic crystal struc-

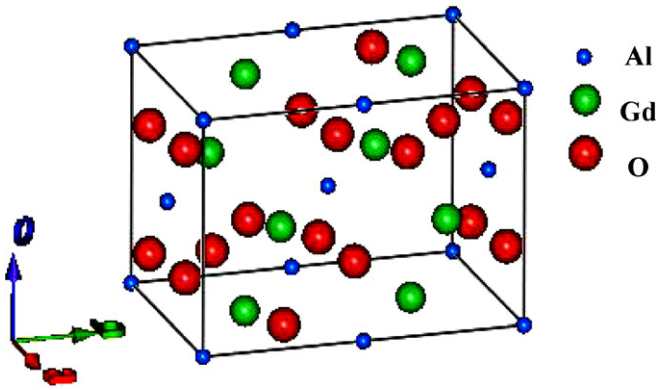

Fig. 7. $GdAlO_3$ orthorhombic unit cell ($Z=4$).

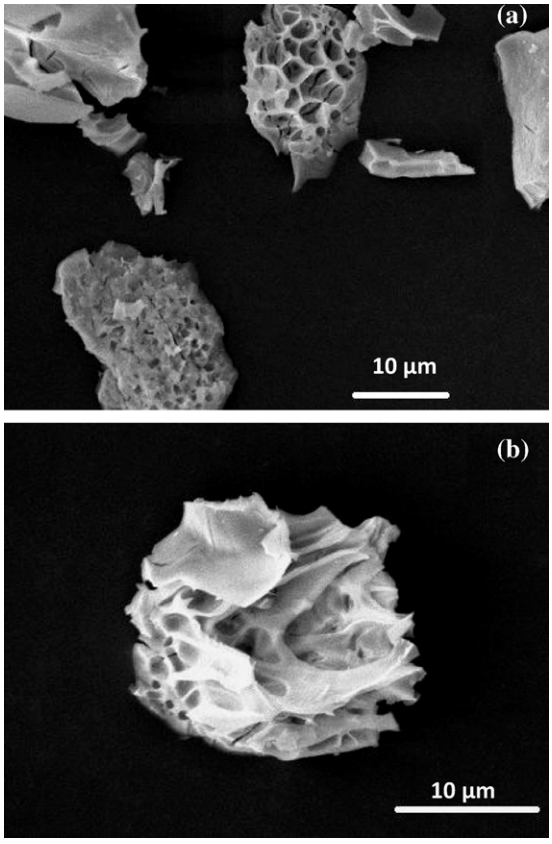

Fig. 8. SEM photomicrographs of $GdAlO_3$ powder calcined at 1000 °C for 2 h.

Table 2
Lattice parameters and cell volume of $GdAlO_3$ phase obtained after Rietveld refinement of XRD data along with similar data from standard pattern of the phase for comparison.

Lattice parameters (Å)/cell volume (Å^3)	$GdAlO_3$ in the present investigation[a]	$GdAlO_3$ ICDD PDF 046-0395	$GdAlO_3$ single crystal [31]
a	5.29883 (7)	5.3017(2)	5.3049(7)
b	7.44594 (9)	7.4450(3)	7.4485 (9)
c	5.25275 (6)	5.2511(3)	5.2537 (6)
Vol.	207.246 (5)	207.27	207.59 (4)

[a] Reliability parameters of the refinement: R_p: 4.62% R_{wp}: 5.80% R_{exp}: 5.18% χ^2: 1.25.

ture of $GdAlO_3$ could be visualised using FpStudio (v 1.0) program of Fullprof Suit [30]. Fig. 7 illustrates the orthorhombic unit cell of perovskite structure of $GdAlO_3$. The $GdAlO_3$ unit cell is distorted due to tilted [AlO_6] cluster octahedra.

3.4. Morphology of $GdAlO_3$ powder

The SEM photomicrographs of $GdAlO_3$ powder calcined at 1000 °C are shown in Fig. 8a and b. The pictures exhibit that the powder was agglomerated and has characteristic shell structure. The shell was porous because of evolution of gases during drying and/or calcination stages. The shell is made up of nano-grains which are partially sintered. The nano-particles/grains have lost their identities. The morphology of powder suggests that it is composed of porous, soft agglomerates containing nanocrystalline grains, which is an important criterion for obtaining good sinterability.

4. Conclusions

Phase pure $GdAlO_3$ powder was prepared through citrate gel route. The decomposition of citrate–nitrate precursor powder was found to be a three-step process: (i) evolution of water and ammonia; (ii) evolution of carbon dioxide, residual water, and ammonia; (iii) oxidation of residual carbon. The $GdAlO_3$ phase forms after calcination at 1000 °C for 2 h under static air. In the absence of oxidizing environment, the amorphous powder partially crystallizes into $GdAlO_3$ phase at 1200 °C. The lattice parameters of the calcined powder were determined through Rietveld refinement of high resolution XRD pattern. The $GdAlO_3$ powder obtained after calcination at 1000 °C was found to be porous and soft agglomerated, composed of nanocrystalline grains.

Acknowledgements

The authors wish to thank G. Kaiser of Max-Planck-Institut für Metallforschung, Stuttgart, for TG–DSC–MS and chemical analysis of the powder. One of the authors (A.S.) thanks Deutscher Akademischer Austausch Dienst (DAAD) for financial support in the form of a fellowship.

References

[1] M.J. Jackson, W. O'Neill, J. Mater. Proc. Technol. 42 (2) (2003) 517–525.
[2] L. Vasylechko, A. Senyshyn, U. Bismayer, Handbook Phys. Chem. Rare Earths 39 (2009) 113–295.
[3] B. Jancar, D. Suvorov, M. Valant, G. Drazic, J. Eur. Ceram. Soc. 23 (9) (2003) 1391–1400.
[4] P. Voňka, J. Leitner, J. Solid State Chem. 182 (4) (2009) 744–748.
[5] H. Hayashi, H. Inaba, M. Matsuyama, N.G. Lan, M. Dokiya, H. Tagawa, Solid State Ionics 122 (1999) 1–15.
[6] S.D. Han, S.P. Khatkar, V.B. Taxak, D. Kumar, J.-Y. Park, Mater. Sci. Eng. B 127 (2–3) (2006) 272–275.
[7] J.Y. Park, H.C. Jung, G.S.R. Raju, B.K. Moon, J.H. Jeong, S.-M. Son, J.H. Kim, Mater. Res. Bull. 45 (2010) 572–575.
[8] H.H.S. Oliveira, M.A. Cebim, A.A. Da Silva, M.R. Davolos, J. Alloys Compd. 488 (2010) 619–623.
[9] J.W.M. Verweij, M.Th. Cohen-Adad, D. Bouttet, H. Lautesse, B. Moine, C. Pédrini, Chem. Phys. Lett. 239 (1995) 51–55.
[10] L.M. Qiu, T. Numaxawa, G. Thummes, Cryogenics 41 (2001) 693–696.
[11] A. Sinha, B.P. Sharma, P. Gopalan, Electrochim. Acta 51 (2006) 1184–1193.
[12] A. Sinha, H. Näfe, B.P. Sharma, P. Gopalan, J. Electrochem. Soc. 155 (2008) B309–B314.
[13] G. Cao, Nanostructures and Nanomaterials. Synthesis, Properties and Applications, Imperial College Press, London, 2004.
[14] H.H.S. Oliveira, M.A. Cebim, A.A. Da Silva, M.R. Davolos, J. Alloys Compd. 488 (2009) 619–623.
[15] H. Gao, Y. Wang, J. Lumin. 122–123 (2007) 997–999.
[16] S. Cizauskaite, V. Reichlova, G. Nenartaviciene, A. Beganskiene, J. Pinkas, A. Kareiva, Mater. Chem. Phys. 102 (2007) 105–110.
[17] A. Sinha, B.P. Sharma, Mater. Res. Bull. 32 (11) (1997) 1571–1579.
[18] M.P. Pechini, US Patent 3,330,697 (1967) (July 11).
[19] W. Trakarnpruk, C. Sukkaew, J. Alloys Compd. 460 (2008) 565–569.
[20] C. Georgi, H. Kern, Ceram. Int. 35 (2009) 755–762.
[21] S. Yamamoto, Y. Ohashi, Y. Masubuchi, T. Takeda, T. Motohashi, S. Kikkawa, J. Alloys Compd. 482 (2009) 160–163.
[22] F.P. Yu, D.R. Yuan, X.L. Duan, L.M. Kong, X.Z. Shi, S.Y. Guo, L.H. Wang, X.F. Cheng, X.Q. Wang, J. Alloys Compd. 459 (2008) L1–L4.
[23] F. Deganello, G. Marcì, G. Deganello, J. Eur. Ceram. Soc. 29 (2009) 439–450.
[24] K.P. Lopes, L.S. Cavalcante, A.Z. Simões, J.A. Varela, E. Longo, E.R. Leite, J. Alloys Compd. 468 (2009) 327–332.
[25] A. Sinha, B.P. Sharma, P. Gopalan, H. Näfe, J. Alloys Compd. 492 (2010) 325–330.
[26] T. Roisnel, J. Rodríguez-Carvajal, in: R. Delhez, E.J. Mittemeijer (Eds.), Proceedings of the Seventh European Powder Diffraction Conference (EPDIC 7), 2000, pp. 118–123.
[27] P. Thompson, D. Cox, J. Hastings, J. Appl. Cryst. 20 (1987) 79–83.
[28] R.A. Young, The Rietveld Method, Oxford University Press, Oxford, 1993.
[29] V.K. Pecharsky, P.Y. Zavalij, Fundamentals of Powder Diffraction and Structural Characterization of Materials, Springer, 2005.
[30] Fullprof. Suite program available at http://www.llb.cea.fr/fullweb/fp2k/fp2k.htm.
[31] D.D. Boulay, N. Ishizawa, E.N. Maslen, Acta Cryst. C60 (2004) i120–122.